



ÄSPÖLABORATORIET

**INTERNATIONAL
COOPERATION
REPORT**

94-03

**The Multiple Well Tracer Experiment -
Scoping calculations**

Urban Svensson
Computer-Aided Fluid Engineering

March 1994

Supported by SKB, Sweden

102.8

SVENSK KÄRNBRÄNSLEHANTERING AB
SWEDISH NUCLEAR FUEL AND WASTE MANAGEMENT CO
BOX 5864 S-102 40 STOCKHOLM
TEL. +46-8-665 28 00 TELEX 13108 SKB TELEFAX +46-8-661 57 19

9505040341 950424
PDR WASTE PDR
WM-11

ISSN 1104-3210
ISRN SKB-ICR--94/3--SE

*Perd well letter dtd
4/25/94*

THE MULTIPLE WELL TRACER EXPERIMENT - SCOPING CALCULATIONS

Urban Svensson

Computer-Aided Fluid Engineering

March 1994

Supported by SKB, Sweden

This document concerns a study which was conducted within an Äspö HRL joint project. The conclusions and viewpoints expressed are those of the author(s) and do not necessarily coincide with those of the client(s). The supporting organization has reviewed the document according to their documentation procedure.

**THE MULTIPLE WELL TRACER EXPERIMENT
- SCOPING CALCULATIONS**

by

**URBAN SVENSSON
COMPUTER-AIDED FLUID ENGINEERING**

1994-03-18

ABSTRACT

A field experiment on flow and transport in a single fracture, called the Multiple Well Tracer Experiment (MWTE), is currently under planning. The report provides scoping calculations for this experiment.

The mathematical model is based on the three-dimensional Navier-Stokes equations which are solved in a body-fitted, to follow the aperture variations, coordinate system. A Lagrangian technique is used for transport of matter. The aperture field is generated from the cubic law and a transmissivity field with given statistics.

The main result of the report is perhaps that a realistic model of flow and transport in a single fracture has been developed. It is however hoped that the results presented will also be of direct interest and use in the planning of the MWTE.

ABSTRACT (SWEDISH)

För närvarande planeras ett projekt, kallat "Multiple Well Tracer Experiment (MWTE)", vilket rör flöde och transport i en enskild bergsspricka. Denna rapport avser att, genom matematisk modellering, ge underlagsinformation till detta experiment.

Den matematiska modellen baseras på Navier-Stokes ekvationer, vilka löses i ett randanpassat koordinatsystem för att kunna följa sprickviddsvariationer. Sprickgeometrin genereras från kubiska lagen och antagna statistiska egenskaper hos transmissivitetsfältet.

Det väsentligaste resultatet i rapporten är kanske att realistiska beräkningar av problemet kan genomföras. Förhoppningsvis ger dock resultaten som presenteras i rapporten även en ökad förståelse för aktuella fysikaliska processer, vilket kan vara av värde i experimentplaneringen.

TABLE OF CONTENTS

		Page
1	INTRODUCTION	1
2	MATHEMATICAL MODEL	3
2.1	BASIC ASSUMPTIONS	3
2.2	FRACTURE GEOMETRY	3
2.3	FLOW MODEL	4
2.4	TRACER TRANSPORT	4
3	RESULTS	5
3.1	COMPUTATIONAL DETAILS	5
3.2	HYDRAULICS	5
3.3	TRACER TRANSPORT AND DISPERSION	12
3.4	APERTURE CHARACTERIZATION	18
4	DISCUSSION	23
5	CONCLUSIONS	26
6	REFERENCES	27
	APPENDIX A	28
	MULTIPLE WELL TRACER EXPERIMENT	
	GENERIC ASSUMPTIONS OF FRACTURE	
	GEOMETRY FOR SCOPING CALCULATIONS	
	APPENDIX B	
	DOCUMENTATION OF HARDWARE AND	
	SOFTWARE	

INTRODUCTION

The objective of the Multiple Well Tracer Experiment (MWTE) is to test the validity of the different conceptual and numerical models of tracer transport in a single fracture (Olsson (1993)). A relatively large number of boreholes, of the order ten, will be drilled through the fracture, enabling various tracer transport and hydraulic tests. The processes and parameters of interest include dispersion, matrix diffusion, sorption, scale effects, etc.. For further details, see Olsson (1993).

The purpose of the present report is to provide scoping calculations of the MWTE. It is the intention to discuss flow and transport in a fracture in a rather fundamental way, in order to increase our understanding of the processes involved. It is further the intention to provide background information for the experimental design.

A schematic outline of the problem is given in Figure 1. A tracer injected at time $t = 0$ will at a later time, $t = t_1$, be at a different position and the "cloud" will also have a different shape and volume. The task is to understand and predict the transport and dispersion of the tracer. Obviously the first task is to predict the flow field, which will be a function of pressure gradients, width variation of the fracture, presence of flakes in the fracture and of course the properties of the fluid. With a known flow field the tracer transport and dispersion is a function of fluid velocity field, molecular diffusion, sorption and matrix diffusion. The two last mentioned processes will not be dealt with in the present analysis and the tracer is thus assumed to "stay in the water".

The scientific problem is to formulate a mathematical model that includes the processes listed above. Such a mathematical model can then form the basis for a numerical model that can be used for predictions. These are the topics to be discussed next.

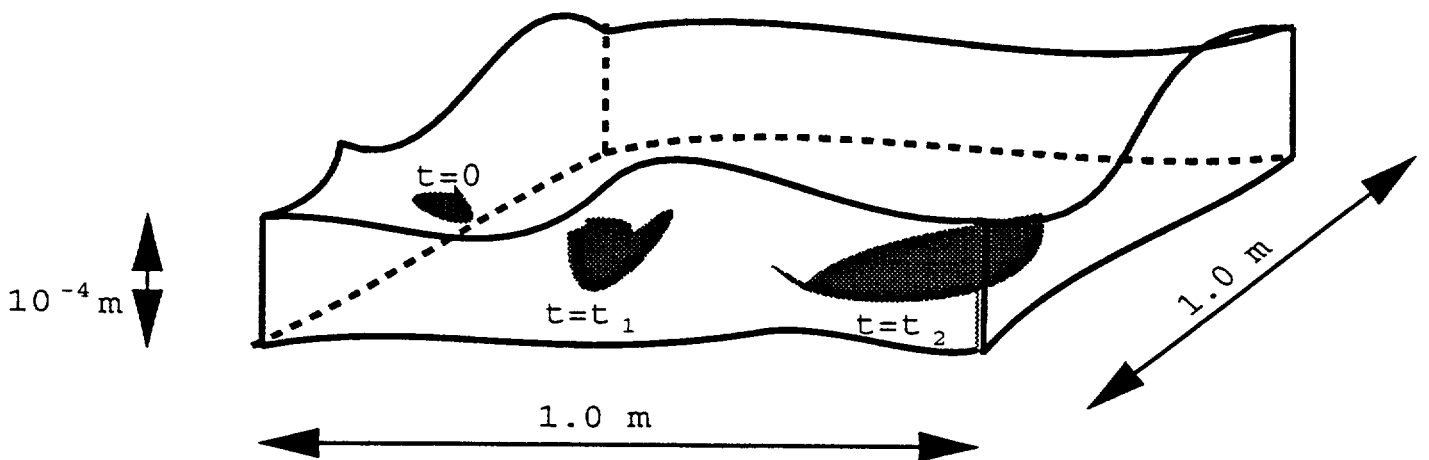


Figure 1. Schematic outline of problem considered.

2 MATHEMATICAL MODEL

2.1 BASIC ASSUMPTIONS

The flow problem will be treated as a laminar three-dimensional flow in a slot of varying aperture. Fluid properties will be assumed to be constant with values relevant for water. Sorption and matrix diffusion will not be dealt with.

2.2 FRACTURE GEOMETRY

The aperture, and its variations, will be calculated by relating the local aperture to the transmissivity by the cubic law. It will be assumed that the transmissivity is \ln normally distributed, with a geometric mean of $3 \times 10^{-7} \text{ m}^2/\text{s}$ and a \ln standard deviation in the range 0.0 to 2.0. The autocorrelation structure of the transmissivity also needs to be considered. It is expected that the correlation length is of the order 0.02 m. An algorithm has been developed, within the project, that generates a matrix of random numbers with a given correlation structure. The algorithm is fully described in Kuylenstierna and Svensson (1993). The user input to the algorithm is illustrated in Figure 2. The three numbers x_0 , y_0 , b , specifies an ellipse and its orientation. The ellipse gives the distance where the correlation is reduced to e^{-1} . Further details, and examples of use, can be found in the reference above. Background to the choice of numerical values can be found in Gustafson (1993), included as Appendix A, where the conceptual model is outlined.

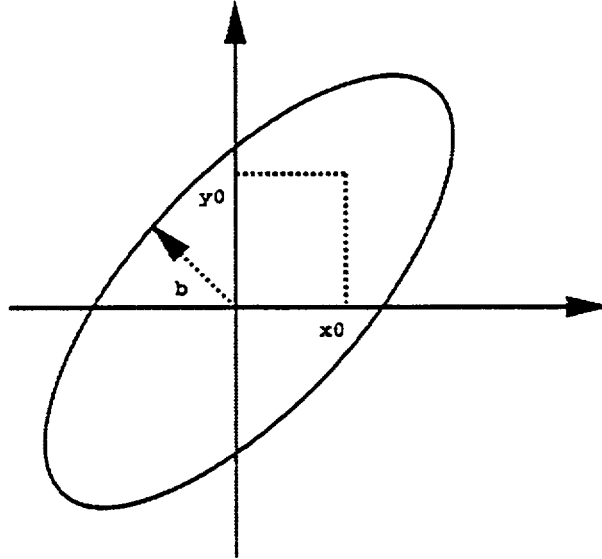


Figure 2. Specification of correlation structure.

2.3 FLOW MODEL

With a given aperture field a three-dimensional body-fitted coordinate (BFC) system can be made to fill the fracture completely. The equation solver used, PHOENICS (Spalding, 1981), has the ability to solve Navier-Stokes equation in such a coordinate system. This facility was used. The equations read:

Navier-Stokes eqn.

$$\frac{\partial u_i u_j}{\partial x_j} = -\frac{1}{\rho} \frac{\partial p}{\partial x_i} + \frac{\partial}{\partial x_j} \left(\nu \frac{\partial u_i}{\partial x_j} \right) ; \quad i = 1,2,3 \quad (1)$$

Mass conservation eqn.

$$\frac{\partial \rho u_i}{\partial x_i} = 0 \quad (2)$$

where p is pressure, ν kinematic viscosity, ρ density, x_i coordinate and u_i velocity. The computational domain covers only half the fracture; a symmetry plane is thus used as one boundary condition and a wall with friction is the other. Fixed pressures are used at the inlet and outlet and a zero-flux condition is used for the two remaining boundaries. Flakes are considered by replacing the symmetry plane, locally, with a wall-condition. Flake positions are distributed randomly, with a given total flake area. Further details on the conceptual model of the flake geometry can be found in Gustafson (1993), see Appendix A.

2.4 TRACER TRANSPORT

A Lagrangian approach is used for tracer transport. The tracer cloud is marked by a number of particles, which are tracked through the domain. Brownian motion is included by a random term; thus:

$$X_i^{t+\Delta t} = X_i^t + u_i \Delta t + \Delta X_i' ; \quad i = 1,2,3 \quad (3)$$

where X_i is coordinate, t time, u_i flow velocity, Δt time step and $\Delta X_i'$ the movement due to molecular diffusion. The flow velocity, u_i , is given by the flow model. The random term, $\Delta X_i'$, is independent of the flow velocity and also of coordinate direction. It can be shown that $\Delta X_i'$ gives the expected diffusional spread if $\Delta X_i'$ has a Gaussian distribution with zero mean and standard deviation $\sigma_{\Delta X} = \sqrt{2D_{mol}\Delta t}$, where D_{mol} is the molecular diffusion coefficient for the tracer.

3 RESULTS

3.1 COMPUTATIONAL DETAILS

The dimensions of the computational domain are 1 x 1 metre and an aperture generated as described above. A grid of $100 \times 100 \times 6$ cells was used. A pressure difference over the domain of 500 Pa is specified. This gives a tracer transit time, from inlet to outlet, of the order 10^4 seconds.

Further details are given when results are presented.

3.2 HYDRAULICS

The first case to be discussed deals with the variation of the effective transmissivity with the \ln standard deviation, σ , of the local transmissivity. For this case it is assumed that no flakes are present and that the correlation length for transmissivities, λ , is zero. The result is shown in Figure 3. The effective transmissivity is found to increase with σ . A typical fracture geometry and flow field is given in Figure 4. In order to see the flow field the lower right corner has been magnified and hence only an area of 33×33 cells is shown. The flow vectors in Figures 4 to 8 give the flow ($\text{m}^3/\text{m}, \text{s}$) in layer 3, which is in the middle of the fracture. A scale has not been included and the vectors are thus only intended to give a qualitative picture of the flow field.

Next the effect of flakes will be added. In Figure 5 flow and geometry, for conditions as above but with 20% flakes, are shown. The flakes are found to reduce the flow rate by about 20%, while the pattern is about the same as without flakes. In Figure 6 the direction of the pressure gradient has been altered 90 degrees. By comparing the result with what is shown in Figure 5, it is found that a high local transmissivity is not always related to a high flow rate as both a pressure gradient and a good connectivity are also required.

Using the same fracture geometry, including the flakes, as above a situation with pumping is next considered. Boundary conditions for this case are specified as fixed pressure at left, see Figure 7, boundary and zero flux conditions at right, high and low boundary. A pumprate of $10^{-8} \text{ m}^3/\text{s}$ was specified at a point in the lower right corner. The result can be studied in Figure 7.

Finally a case with an isotropic correlation length, λ , of the order 0.04 metres is to be presented. The fracture geometry is thus specified by this correlation length, $\sigma = 2.0$ and 20% randomly distributed flakes. Pressure gradient is from left to right in Figure 8, where the result can be studied. It is seen that there is a good hydraulic connection between the pressure boundaries in the lower part of the domain and hence we find the high flow rates here.

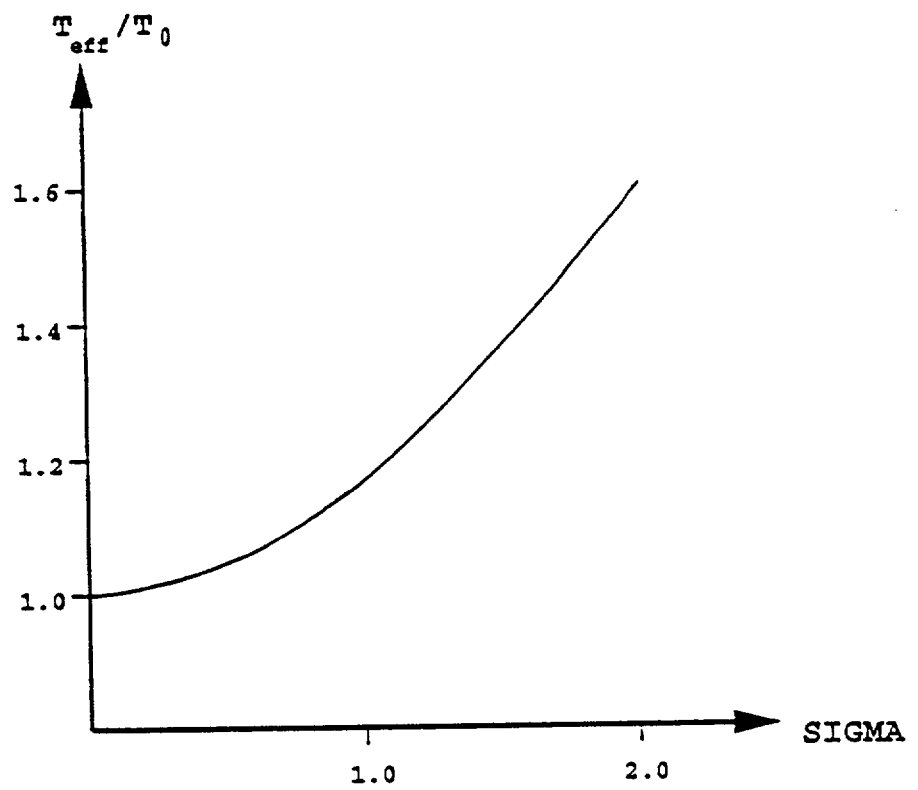


Figure 3. Variation of effective transmissivity with ln standard deviation of local transmissivity, σ . T_0 is the transmissivity for $\sigma = 0$.

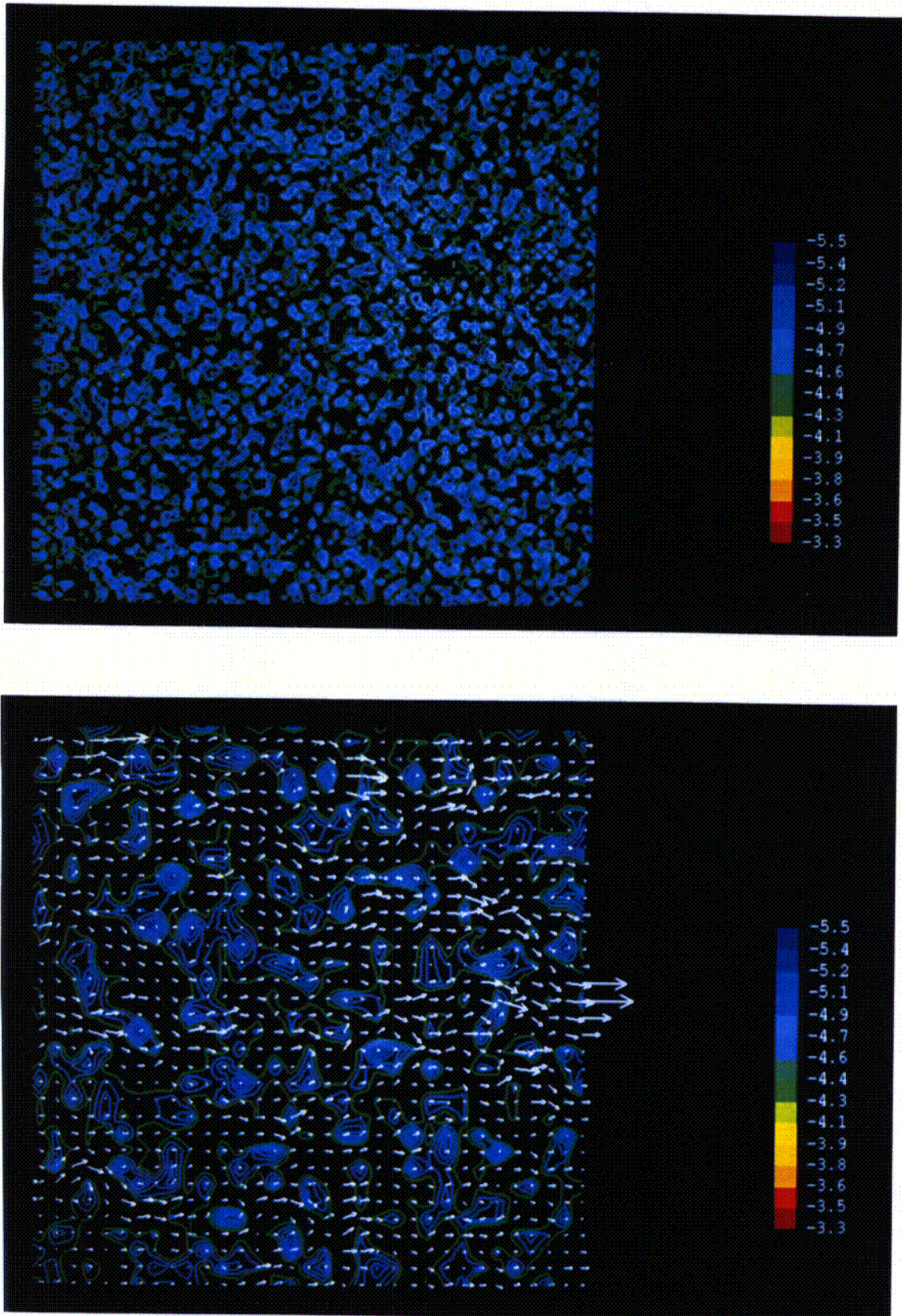


Figure 4. Flow and fracture geometry for no flakes, $\lambda = 0.0$ m and $\sigma = 2$. Scale for width is $_{10}\log$ of actual width.

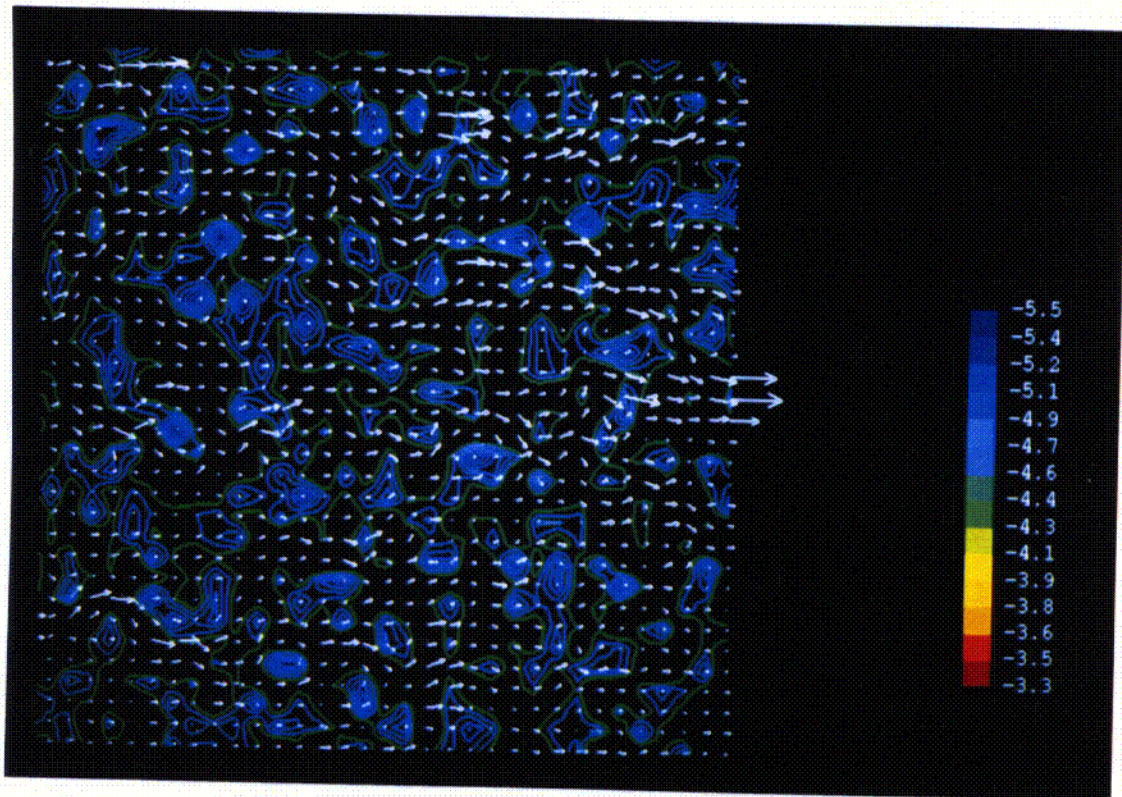


Figure 5. Flow and fracture geometry for $\lambda = 0.0$ m, $\sigma = 2.0$ and with 20% flakes randomly distributed.

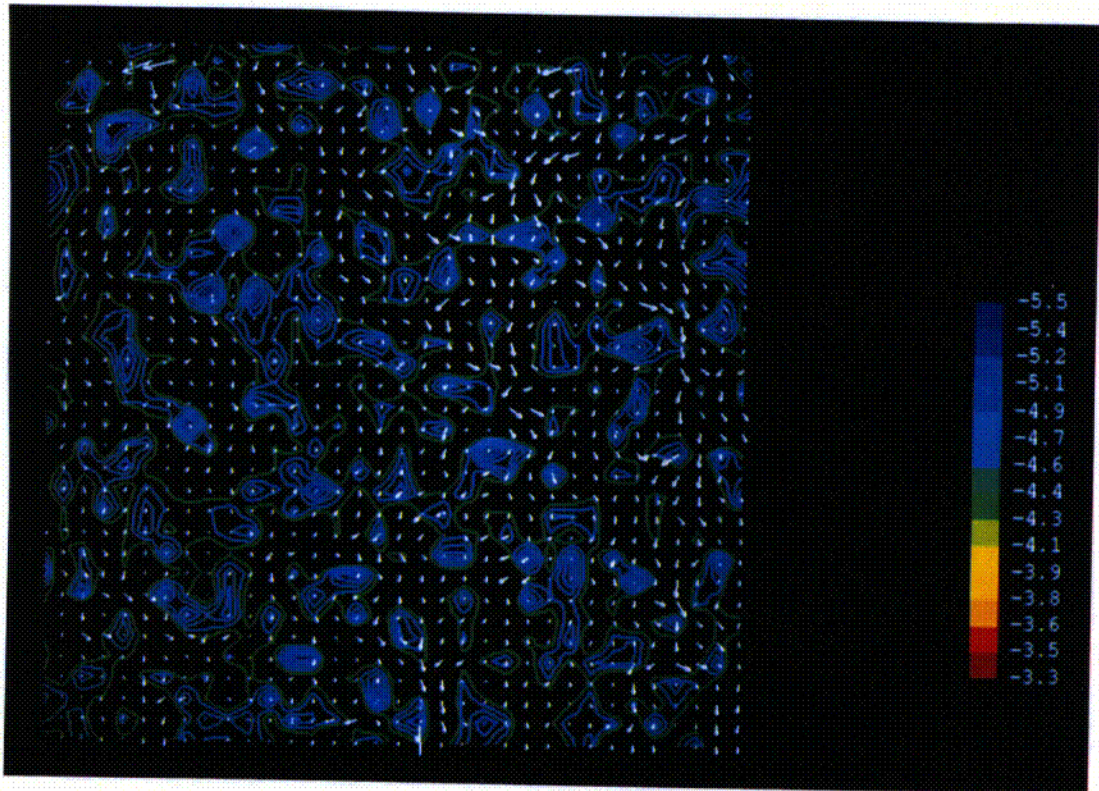


Figure 6. Same condition as for Figure 5, but with direction of pressure gradient altered 90 degrees.

c3

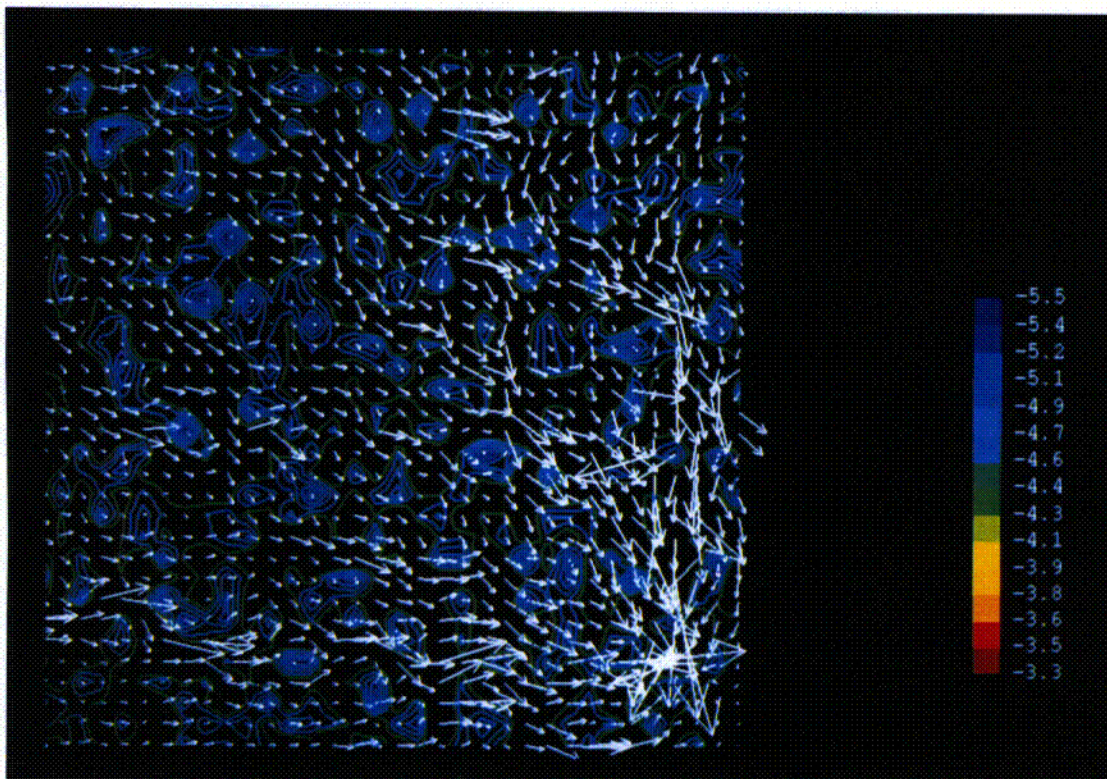


Figure 7. Flow field when pumping in lower right corner. Fracture geometry as for Figure 5.

c4

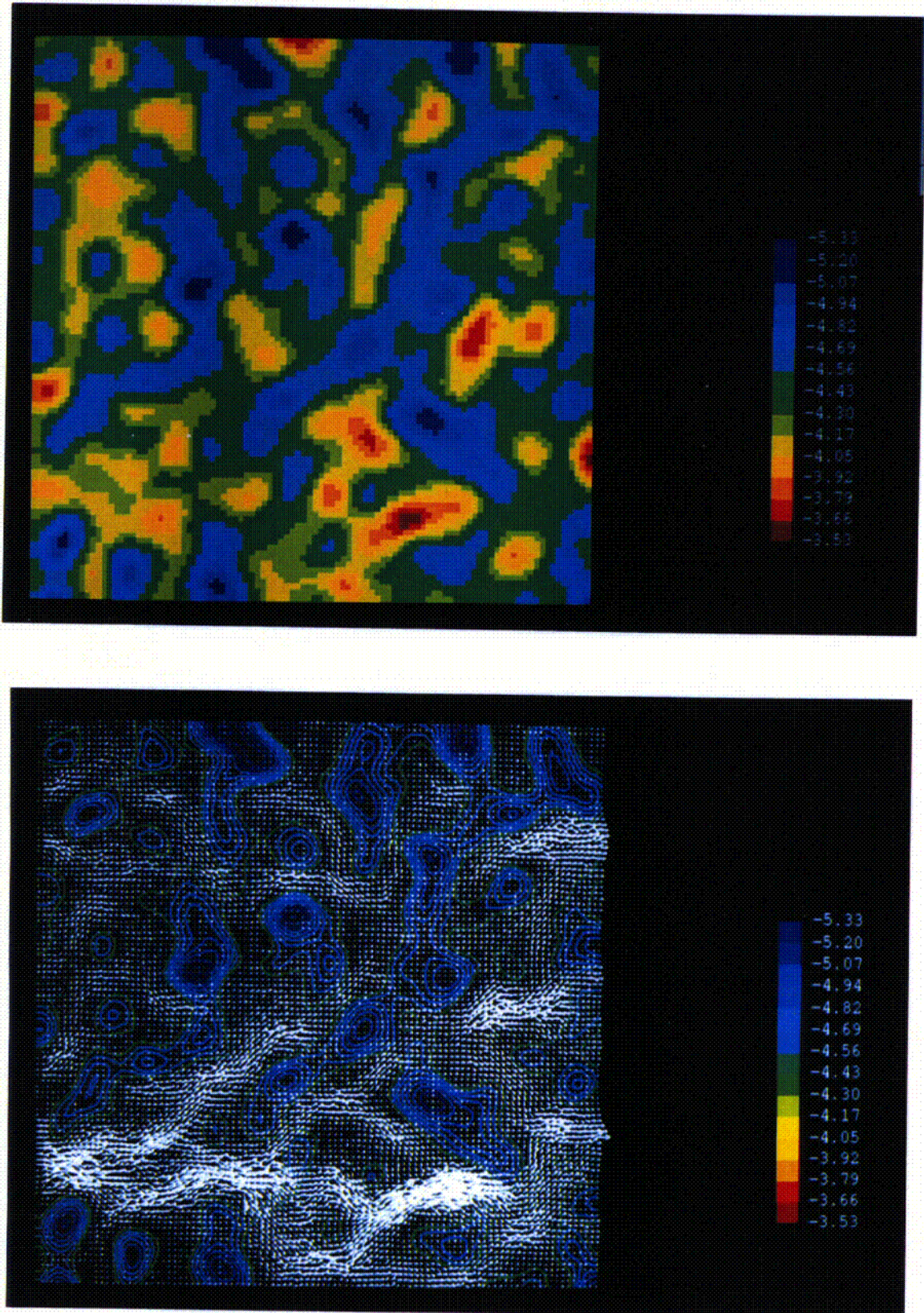


Figure 8. Flow and fracture geometry for $\sigma = 2$, $\lambda = 0.04$ m and 20 % flakes.

C5

TRACER TRANSPORT AND DISPERSION

The predictions to be presented have been carried out with several purposes: test/verify the method used, build up an understanding of the dispersion process and provide background information for the MWTE.

The first thing to establish was that pure molecular diffusion is given by equation (3). Using 500 particles it was found that the correct dispersion coefficient, which is equal to the diffusion coefficient in the uniform flow field used, was obtained to within $\pm 10\%$ for a range of molecular diffusivities.

In a non-uniform flow field hydrodynamical dispersion will be an important process. The process has been studied by many authors (Yasuda (1984), Taivassalo and Hautojärvi (1991)) since the classical work by Taylor (1953). In the present report the analytical solutions by Yasuda (1984) will be used for a comparison with results from the particle tracking method. Yasuda (1984) prescribed the velocity profile, see Figure 9, and found the corresponding dispersion coefficient, which is also a function of the mean velocity, the aperture and the molecular diffusion coefficient. Predictions with the particle tracking algorithm were carried out for the same conditions and the result is in Figure 9 compared with the analytical solutions by Yasuda (1984). As can be seen a good agreement is obtained already for 500 particles, which is the number of particles used.

Next we consider a fracture with variable aperture. The flow field used corresponds to a fracture geometry with $\sigma = 2$, $\lambda = 0.02$ m and 20% flakes. Three different cases will be presented:

- Point source, $D_{mol} = 10^{-10} \text{ m}^2/\text{s}$
- Line source, $D_{mol} = 10^{-10} \text{ m}^2/\text{s}$
- Point source, $D_{mol} = 10^{-11} \text{ m}^2/\text{s}$

The line source is intended to simulate a more realistic injection procedure, as the length of the line, 76 mm, corresponds to the diameter of a borehole. The alternative diffusion coefficient is intended to illustrate the importance of shear dispersion. It should be mentioned that a number of other cases can be, and ought to be, studied with the model set-up. The relation between the dispersion coefficients and the fracture characteristics is one obvious case. These studies have however to be postponed due to time limitations. Results of calculations are shown in Figure 10, 11 and 12.

Starting with Figure 10 we have the point source with $D_{mol} = 10^{-10} \text{ m}^2/\text{s}$. The particles are released at the left, inlet, boundary and will leave at the right boundary. The top figure shows the cloud three hours after release and we can see that the cloud is about to leave the domain. The lower figure shows the particles at

five different times, giving an impression of a continuous release. In this figure the release point can be identified. Corresponding results for the line source can be studied in Figure 11 and the case with $D_{mol} = 10^{-11} \text{ m}^2/\text{s}$ in Figure 12. The lower diffusion coefficient gives a larger longitudinal dispersion which is expected from the analytical work by Yasuda (1984).

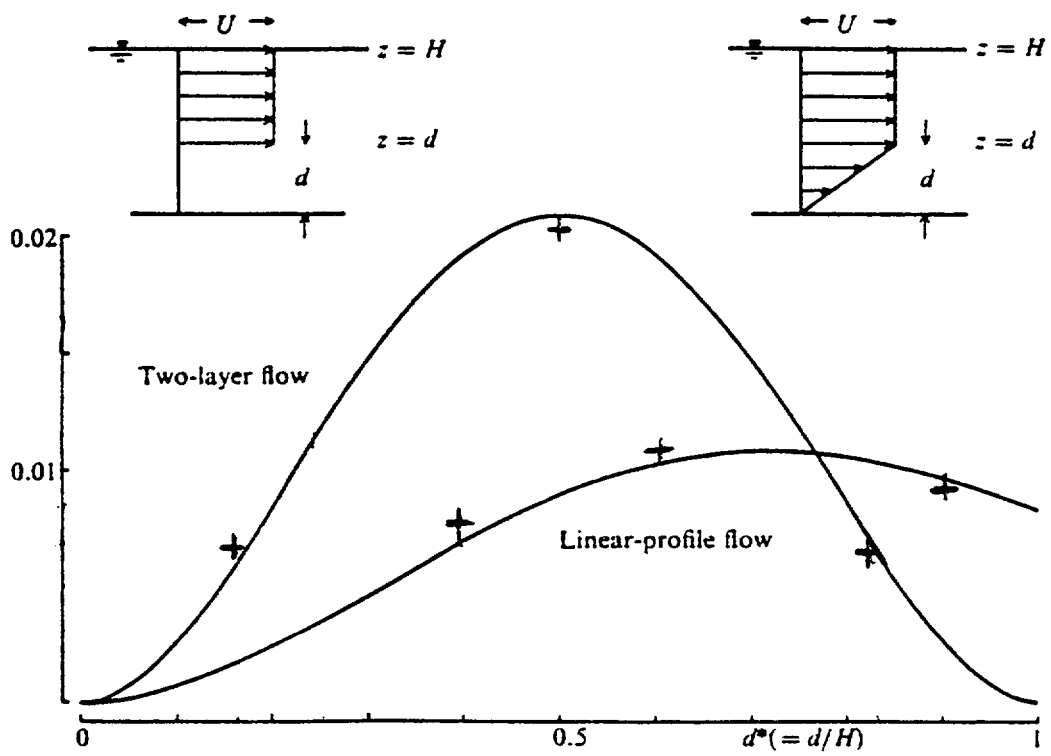


Figure 9. Hydrodynamical dispersion. Comparison between present predictions (crosses) and the analytical solution by Yasuda (1984). Basic figure from Yasuda. The dispersion coefficient is obtained by multiplying the number on the vertical axis by $U^2 H^2 / D_{mol}$.

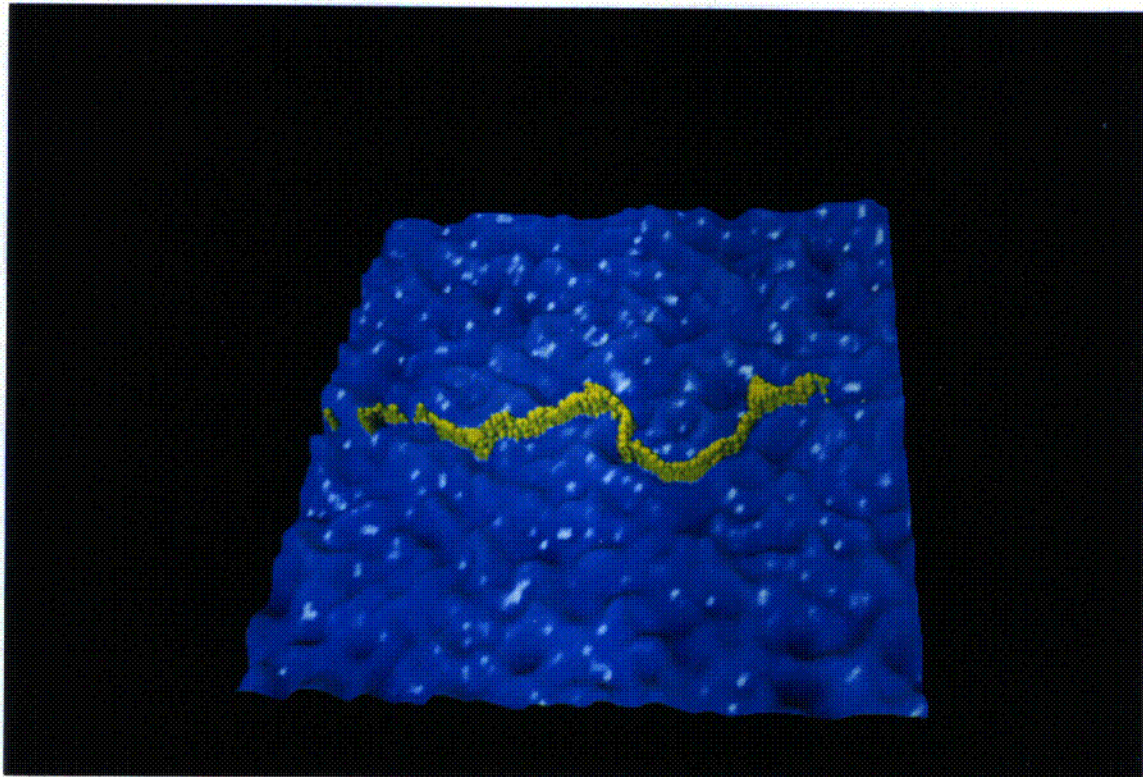
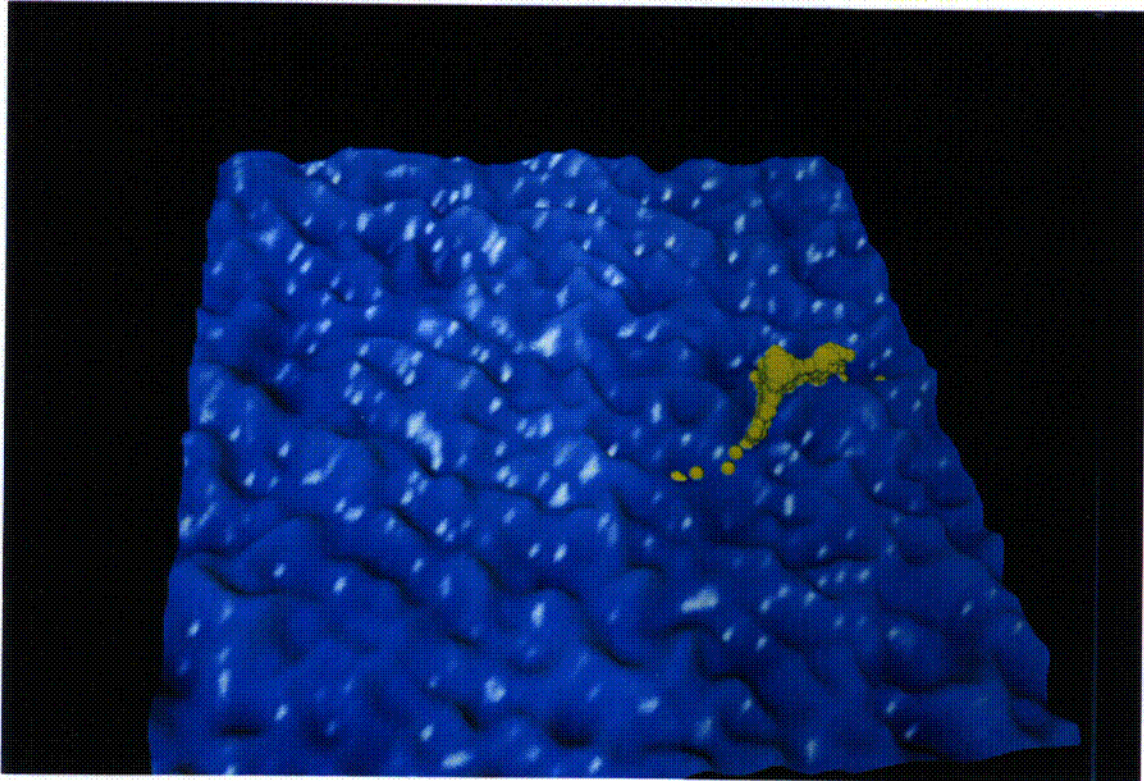


Figure 10. Tracer transport, $D_{mol} = 10^{-10} \text{ m}^2/\text{s}$, point source. Top figure three hours after release, lower figure five different time steps.

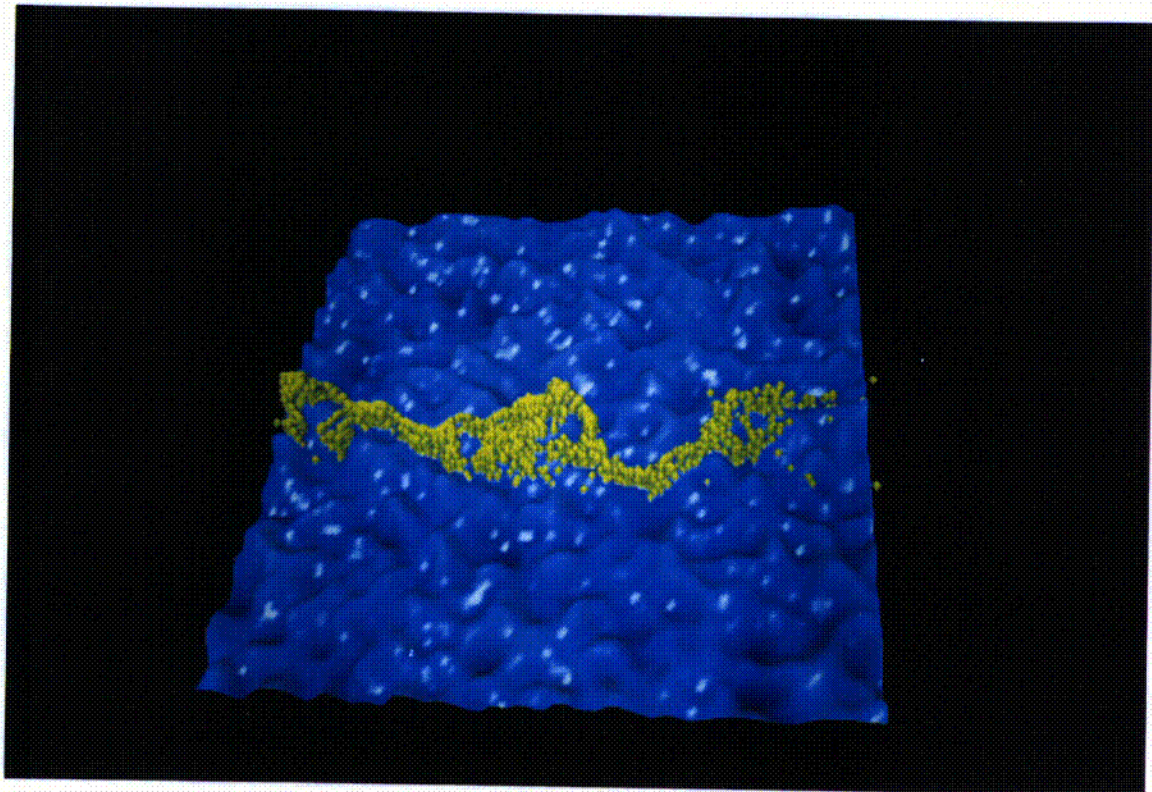
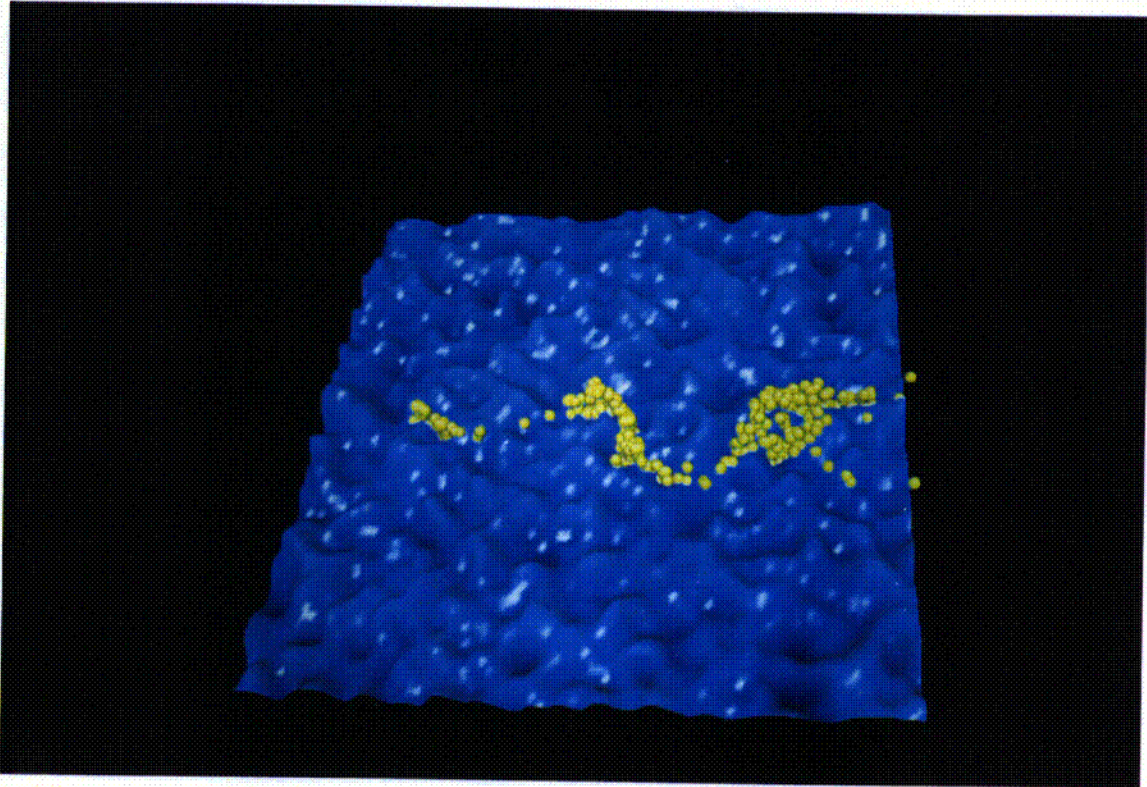


Figure 11. As for Figure 10, but a line source.

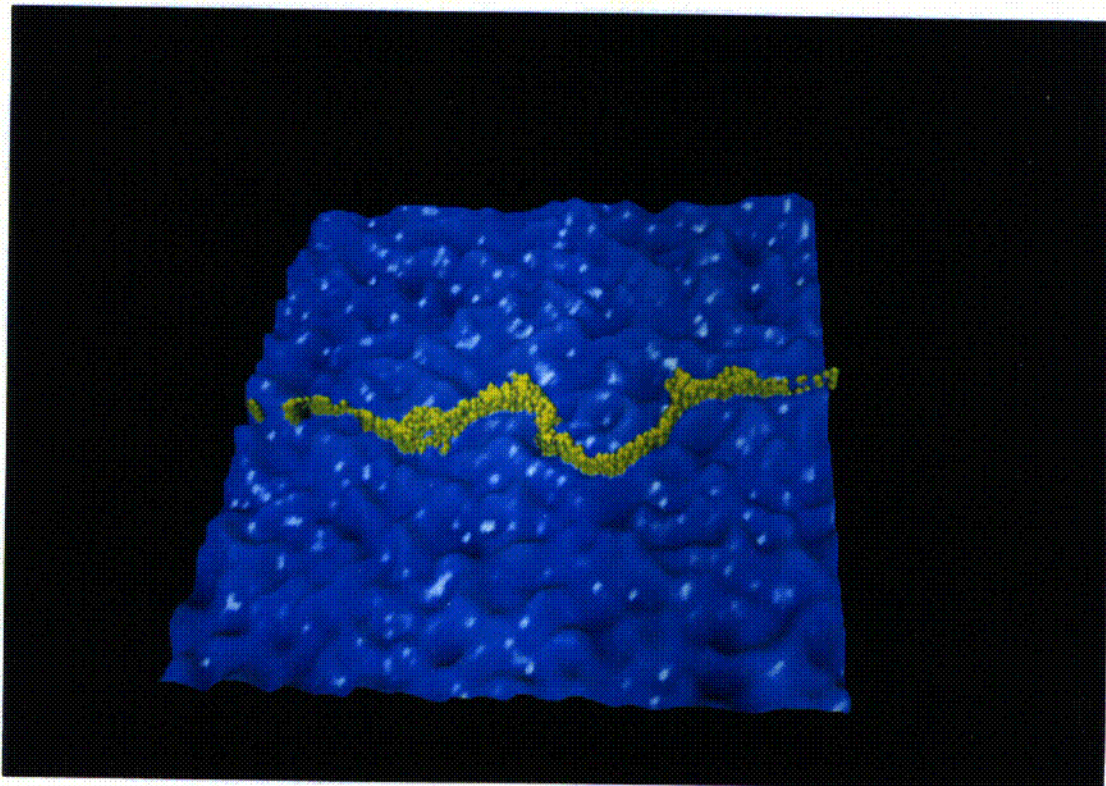
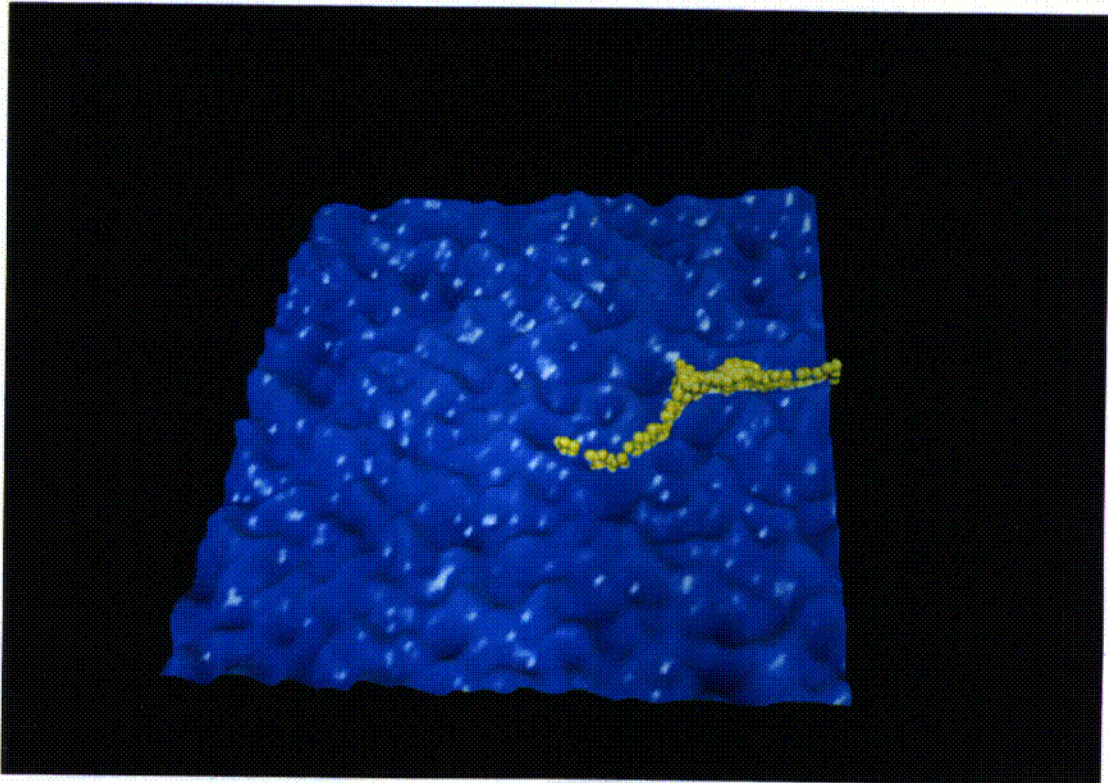


Figure 12. As for Figure 10, but with $D_{mol} = 10^{-11} \text{ m}^2/\text{s}$.

3.4 APERTURE CHARACTERIZATION

As can be seen from the flow fields shown above there are large areas in the fracture plane that contribute insignificantly to the total flow. The importance of processes like sorption and matrix diffusion is related to the contact area between the flow and the matrix and it is thus of interest to characterize the flow and the fracture in these respects.

The most obvious parameters that characterize the fracture are the total pore volume, V_p , and the average aperture, d_p .

$$V_p = \int_A d(x,y) dA \quad (4)$$

$$d_p = V_p / (BL) \quad (5)$$

where $d(x,y)$ is the local aperture, B and L are the dimensions in the fracture plane.

The so called kinematic pore volume, V_k , can be estimated if an average flow time, θ_m , can be obtained:

$$V_k = Q\theta_m \quad (6)$$

$$d_k = V_k / (BL) \quad (7)$$

where d_k is called the kinematic aperture. The average flow time can be obtained by calculating the median transit time for a tracer that passes the fracture.

It is also possible to define an aperture from the cubic law. This aperture, here called the conductive aperture, d_c , is obtained from:

$$d_c = \sqrt[3]{\frac{12Q\nu}{Bgi}} \quad (8)$$

where g is the gravitational acceleration, ν kinematic viscosity and i hydraulic head gradient.

In Table 1 these apertures are estimated for some typical fracture parameters. The flow time, θ_m , was estimated with the particle tracking method described above.

At the inlet 500 particles, with a molecular diffusion coefficient of $D_{mol} = 10^{-10} \text{ m}^2/\text{s}$, were distributed uniformly along the whole of the inlet boundary. The time when 250 particles had passed the outlet gives θ_m . Also the time distribution of arrival times, the break-through curve, was stored. Examples of break-through curves are given in Figures 13 and 14. Coming back to Table 1, we find that the average aperture, d_p , is always the largest. This is to be expected as the two others, when multiplied with a length, represent the area where the flow takes place. It is also noted that d_c is equal for $\lambda = 0.02 \text{ m}$ and 0.04 m . Referring to equation (8) we see that this means that Q was the same for these two cases, which is a pure coincidence. It does however point to the fact that the fracture geometry is only one realization of a stochastic process and that another realization probably would have resulted in a different Q . This effect becomes particularly important when the correlation length increases as the connectivity between the inlet and the outlet will be more variable then.

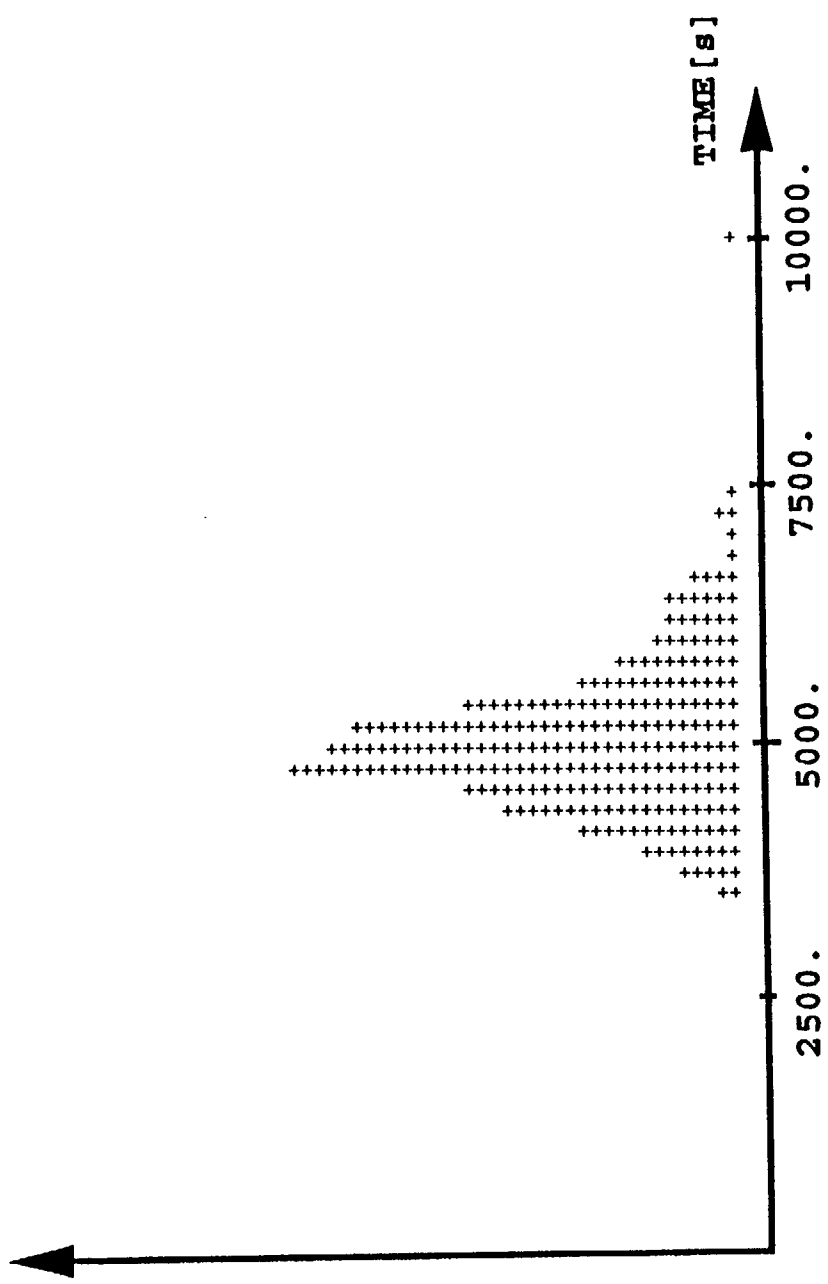
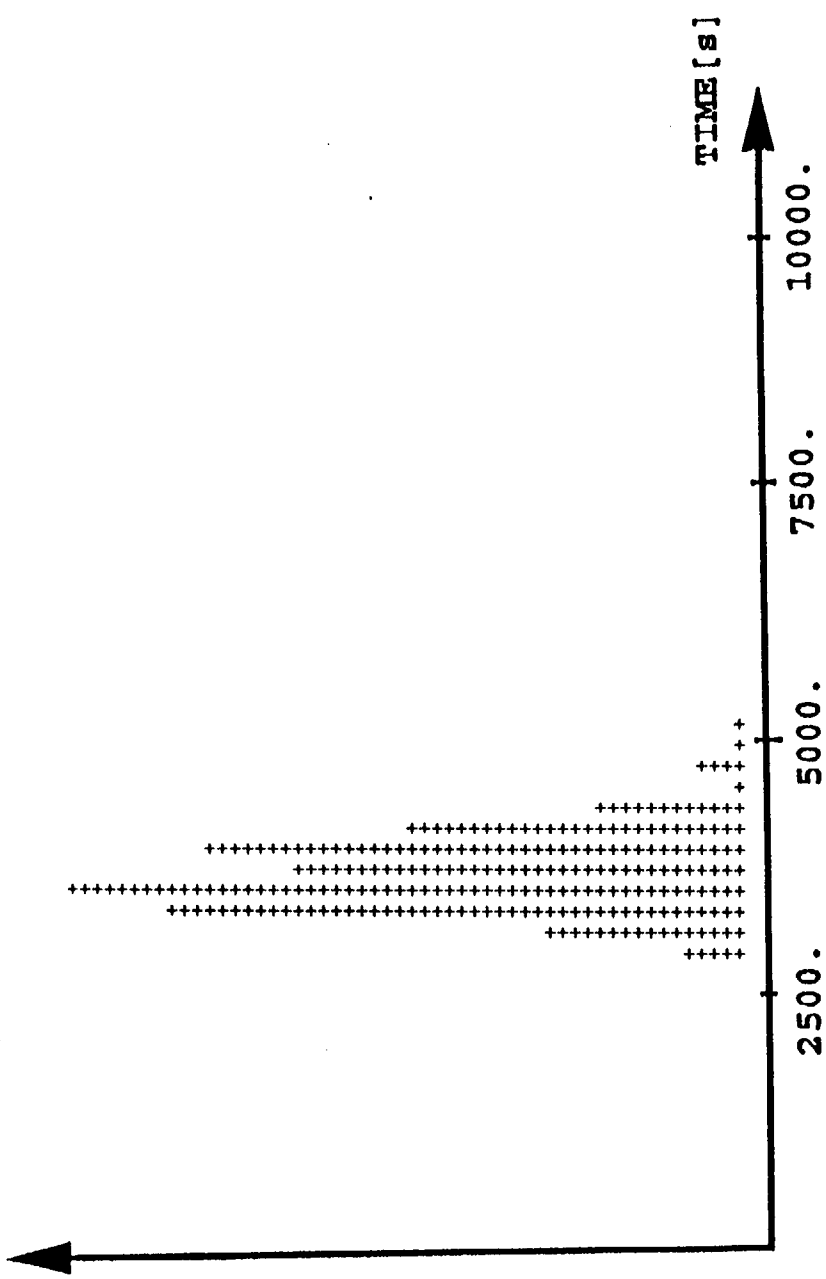


Figure 13. Break-through curves for the cases one (top) and two, as listed in Table 1.

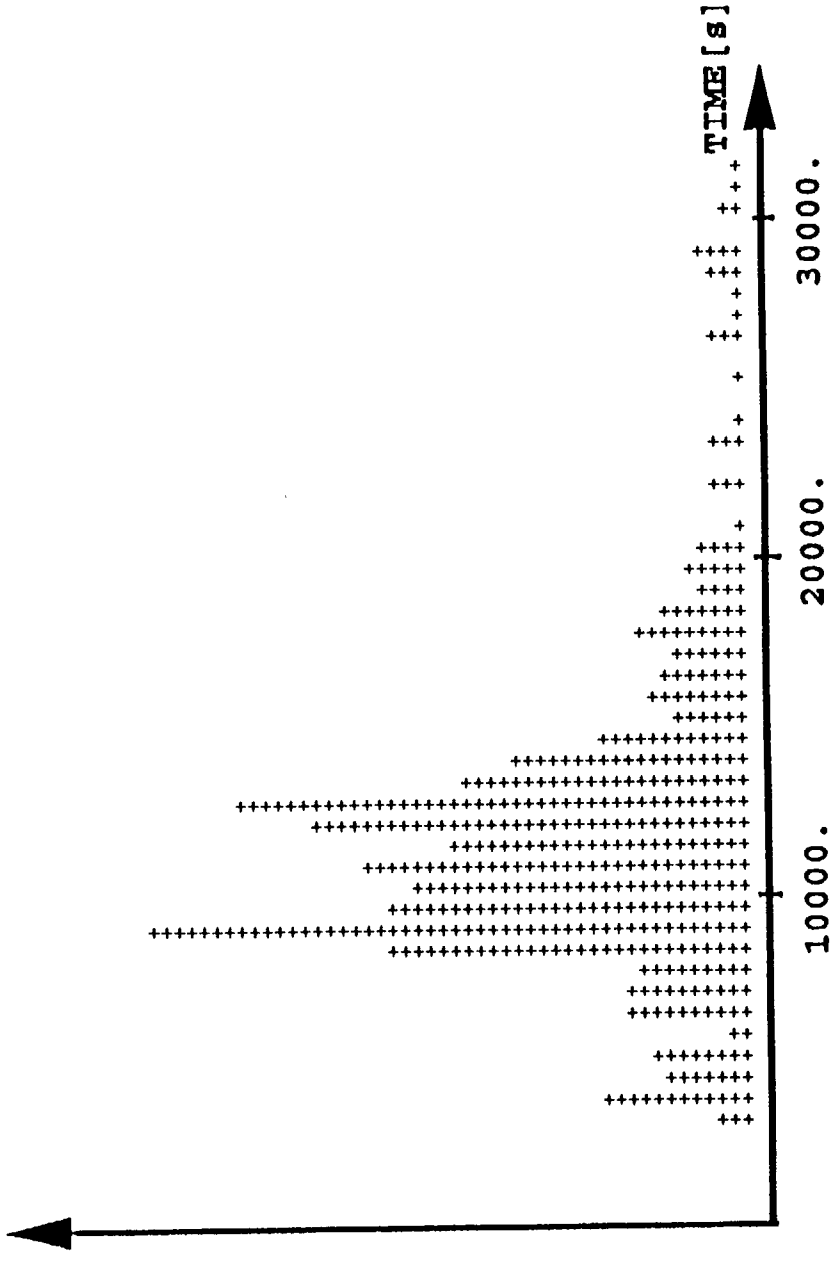
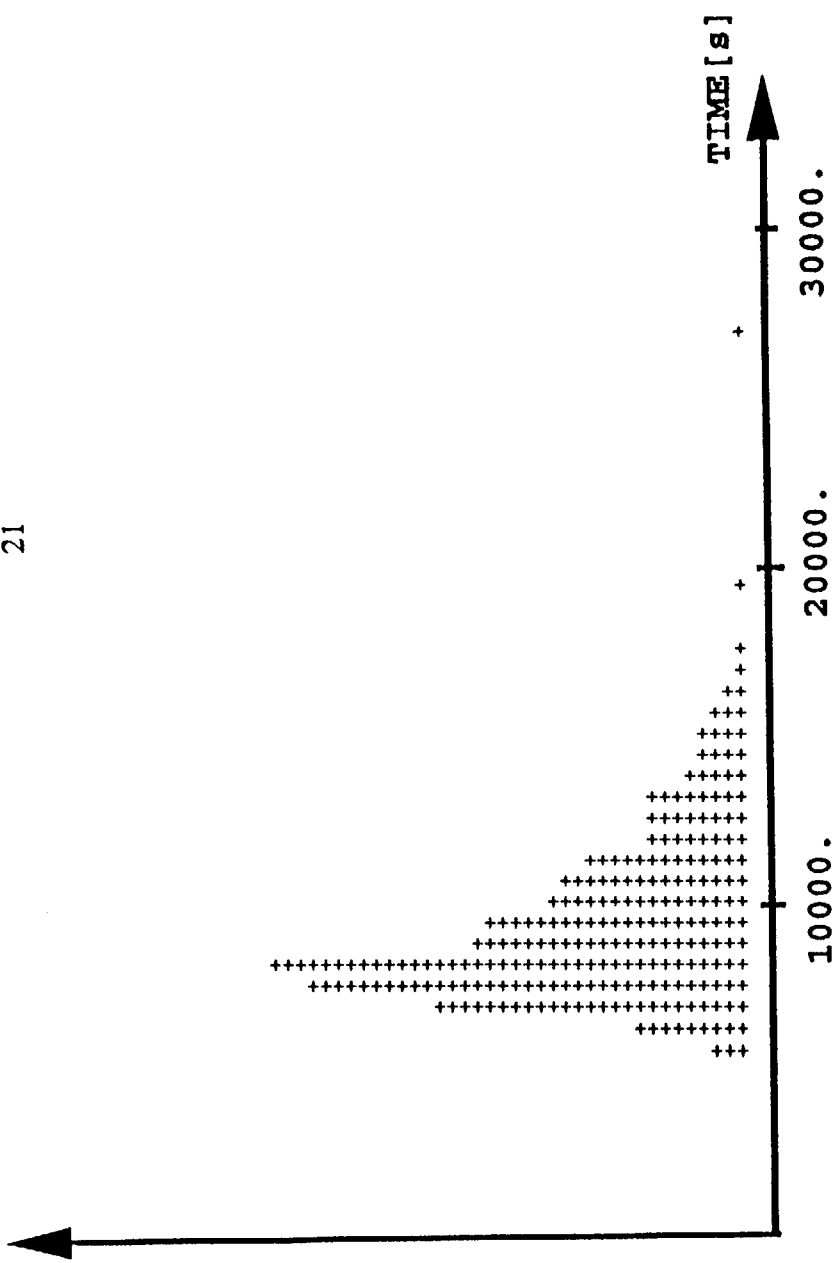


Figure 14. Break-through curves for cases three (top) and four, as listed in Table 1.

Case	$d_p \times 10^5(\text{m})$	$d_k \times 10^5(\text{m})$	$d_c \times 10^5(\text{m})$
$\sigma = 2.0, \lambda = 0.0\text{m},$ $F = 0.0$	17.8	9.0	8.4
$\sigma = 2.0, \lambda = 0.0\text{m},$ $F = 20\%$	17.8	9.5	7.8
$\sigma = 2.0, \lambda = 0.02\text{m},$ $F = 0.0$	18.1	10.4	6.6
$\sigma = 2.0, \lambda = 0.04\text{m},$ $F = 20\%$	17.9	13.7	6.6

Table 1. Various aperture parameters for a range of fracture parameters like \ln standard deviation of transmissivity (σ), correlation length (λ) and percentage flakes (F).

DISCUSSION

If a tracer is injected as a point source at the inlet to a fracture, a certain spread will be noted when it reaches the outlet. Dispersion coefficients are used to characterize the spread.

Often the terms longitudinal and transverse dispersion are used to characterize the spread in the main flow direction and the direction perpendicular to the main flow. This can however be misleading as illustrated in Figure 15. At $t = t_2$ it is alright to define D_x and D_y , as indicated above, but at $t = t_3$ we see that D_y increases, not because a spread but because the main streamline changes angle to the cartesian coordinate system. A solution could be to define a local coordinate system based on the velocity vector of the masscentre of the cloud. However at $t = t_4$ we see that also this definition may be inadequate. A definition that picks up the phenomenon we want to study needs to be quite complex; first the streamline of the masscentre needs to be calculated then deviations from the masscentre, along and perpendicular to the streamline, can be used to define longitudinal and transverse dispersion.

Using these definitions of dispersion we ask ourselves what physical processes are responsible for longitudinal and transverse dispersion. In the authors view longitudinal dispersion is due to shear dispersion, also called Taylor dispersion. Transverse dispersion is always present due to molecular diffusion but this is a fairly weak process for the present conditions. If the flow time is of the order 10^4 s and $D_{mol} = 10^{-10}$ m²/s we can estimate the typical transverse spread as $\sqrt{D_{mol} \times t} = 10^{-3}$ m. If the flow in the fracture is conceptualized to take part in a network of discrete channels, see Figure 16, it is straight forward to see that a tracer will be spread due to "division of streamlines". However, for the correlation lengths used in the present study (≈ 0.02 m) this flow pattern does not result. It is more in resemblance with the field of streamlines obtained from the laboratory measurements by Hakami (1989), see Figure 17. The general picture seen is that two streamlines that start close to each other will probably leave the domain close to each other. This means that the volume between the streamlines is "bounded". Still, streamlines may come in close contact, but this will only last for a flowtime that corresponds to a correlation length (≈ 0.02 m) and, again, molecular diffusion is not very effective on these time scales.

To conclude this discussion, it is the authors view that transverse dispersion, as defined above, is not significant for the conditions studied in this report. This means that the tracer will move in a plane defined by the streamline of the masscentre and be dispersed along this streamline by shear dispersion. This view is supported by the calculations illustrated in, for example, Figure 10. Note that in a real field experiment other processes like unsteadiness in the pressure field, wall roughness, injection procedure, etc may cause also transverse dispersion.

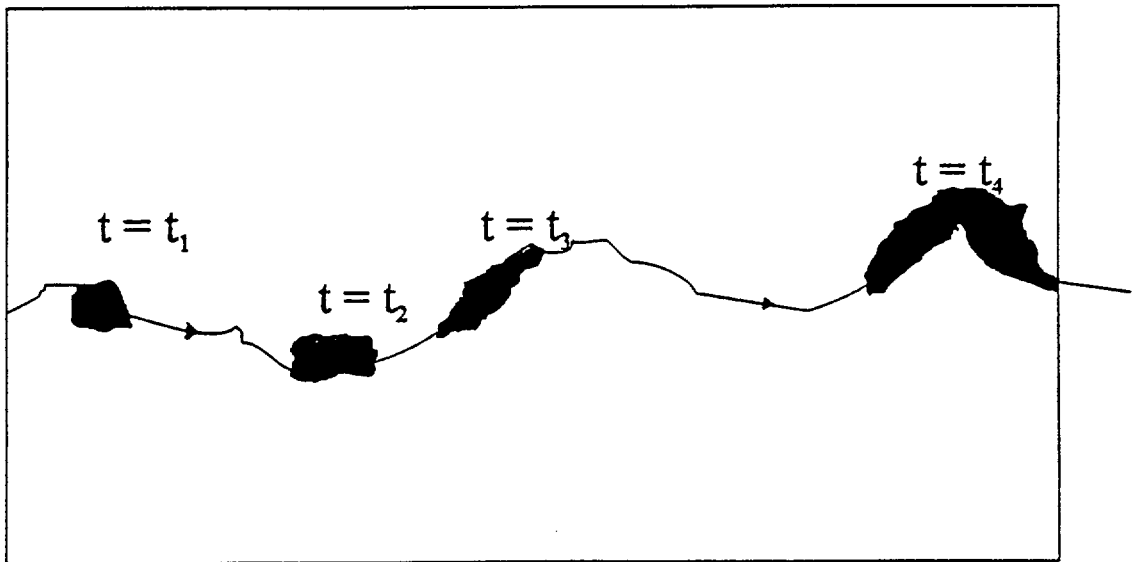


Figure 15. Schematic figure for illustration of dispersion.

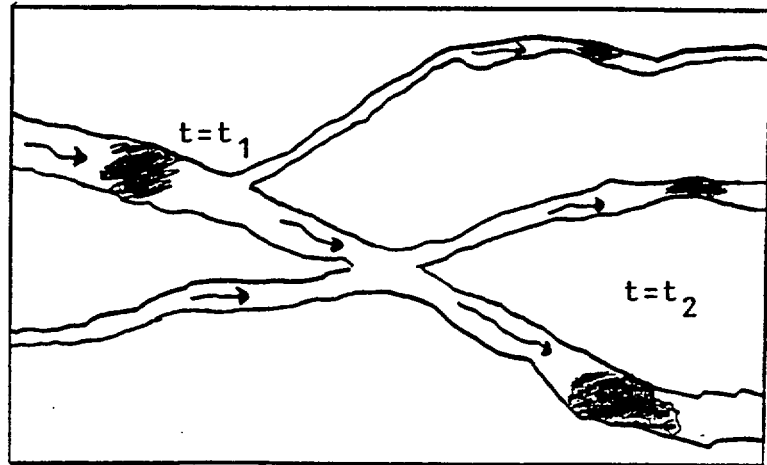


Figure 16. Schematic figure of spread of a tracer in a channel network.

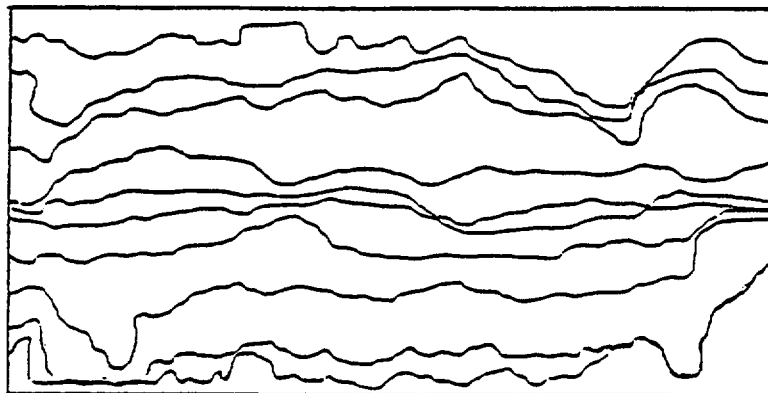


Figure 17. Laboratory measurements of streamlines in a fracture. From Hakami(1989)

CONCLUSIONS

The objective of the work presented has been to provide background information to the MWTE. The chosen approach has been to simulate, by way of mathematical models, the experiment as correctly as possible and, in the process, extract valuable information for the experimental design and objective. It is thus hoped that all results presented will assist in the planning of the MWTE.

It is also worth noting that the project has included development of new methods. The algorithm for fracture geometry generation is expected to be of value in future projects. The flow and transport model is the first fully three-dimensional model (with a BFC-grid) of the problem addressed, as known to the author. When more information is available on fracture aperture distributions it is straight forward to use the models developed to simulate flow and transport in these fractures.

6. REFERENCES**Hakami E.**

Water Flow in Single Rock Joints. Stripa project, TR 89-08. 1989.

Kuylenstierna H-O, Svensson U.

On the numerical generation of fracture aperture distributions. SKB report in preparation. 1994.

Olsson O.

"ÄHRL-Test plans for the operation phase". Material for the Scientific Advisory Committee in Kalmar, Stockholm June 1993.

Spalding D B. A general purpose computer program for multi-dimensional one- and two-phase flow. Math. Comp. Sim., 8, 267-276. 1981.

Taivassalo V, Hautojärvi A.

A novel conceptual model for the flow and transport in fractured rock. Mat. Res. Soc. Symp. Proc. Vol 212. 1991.

Taylor G I.

Dispersion of soluble matter in solvent flowing slowly through a tube. Proc. Roy. Soc. London, 219, 186-203. 1953.

Yasuda H.

Longitudinal dispersion of matter due to the shear effect of steady and oscillatory currents. J. Fluid. Mech. 1984.

APPENDIX A MULTIPLE WELL TRACER EXPERIMENT
Generic Assumptions of Fracture Geometry for Scoping
Calculations

SKB - ÄSPÖ HARD ROCK LABORATORY

**MULTIPLE WELL TRACER EXPERIMENT
Generic Assumptions of Fracture Geometry for Scoping Calculations**

**Gunnar Gustafson
CTH/VBB VIAK**

1 Introduction

A multiple well tracer experiment (MTWE) will be performed in the experiment area of the ÄHRL. The experimental set up will be an array of boreholes penetrating a distinct conductive fracture. In the array a series of flow and migration experiments will be performed. The objectives with the experiments are to evaluate and model proposed conceptual models for nuclide migration in a fractured rock. As a part of the design of the experiment a series of scoping calculations will be carried through in order to find criteria for the choice of a suitable fracture and an appropriate design of the experimental set up. This paper is an effort to summarize a conceptual model for the geometry of a target fracture.

2 The Experiment Area

The plans are to excavate an experiment area immediately South-West of the elevator shaft at full depth, 450 m below sea level. The area will be reached by a bored tunnel with a slight upward slope from the shaft. The area is situated outside the target area of the pre-investigations which is roughly limited to the volume defined by the spiral of the transport tunnel and a rim of about 100 m around that. The experiment area is situated at full depth which limits the available characterization data. A pre-investigation in order to give design information for the bored tunnel and to characterize the experiment area was recently started, but data are not yet available. In the prediction report¹ the properties of two areas close to the shaft are predicted. The best estimate of the conditions at the experiment area is that they will be about the same as for these prediction volumes, P50-09 and P50-10. The reason is that they are closest to the target area, they are at approximately the same depth and they have about the same properties, which indicates reasonably homogeneous conditions.

Both prediction volumes are dominated by Äspö Diorite (> 60%) alternating with Småland Granite and Greenstone. Veins of Fine-grained Granite striking mainly NE - SW occur. Fracturing is most intense in these veins and they are the most conductive parts of the rock. Most frequent fracture groups are N55W/70SE and /35NE, N-S/Steep in this note called NNW-fractures, N85E/75E and /33E and N55E/70E. Median fracture length and spacing in the diorite are estimated to be 1.2 m and 1.0 m respectively.

From the tunnel excavation the N-S group was found to consist of conductive fractures with a substantial length. The median hydraulic conductivity in the 20 m scale is estimated to be slightly more than 10^{-8} m/s. Hydraulic conductors with a transmissivity higher than $T=3 \cdot 10^{-9}$ m²/s occur with a median distance of 7 m and zones with $T > 3 \cdot 10^{-7}$ m²/s occur with median distance of 9 m in boreholes.

The maximum horizontal rock stress is predicted to be directed N40W with the vertical stress and the other horizontal stress about equal.

3 The target fracture

The demands on the experiment volume for the MWTE must as always be a compromise between the desirable and the possible. Primarily the aim of the experiment is to characterize nuclide migration in the good rock, with few fractures and low permeability. Experimental considerations, however, makes it necessary that the tracer tests are performed more or less in one single fracture, where the hydraulics can be controlled and it is not likely that tracers are lost outside the control volume. This demands that a suitable fracture can be identified and characterized by available methods and that the fracture has such an extension that the experiment set up can be achieved with reasonable measures, see Figure 3.1.

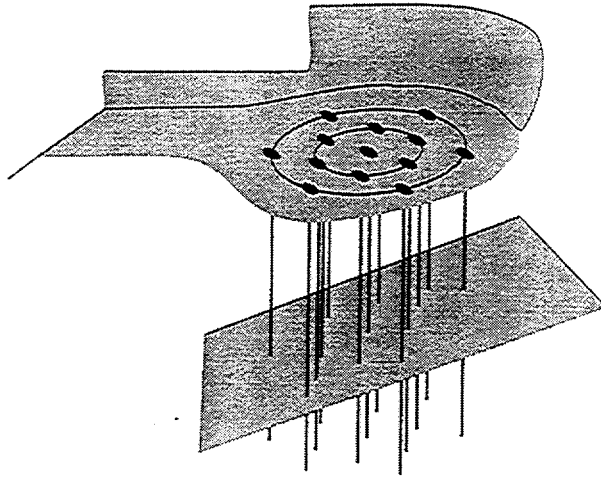


Figure 3.1. The experiment set up for the MWTE²

These demands are not quite compatible with a typical "good" rock but are necessary to fulfil in order to be able to carry through the experiment. Some basic properties of a target can thus be set up such as:

Permeability contrast. It is necessary to identify the fracture by hydraulic means, so we know that we are in a conductive fracture. With the test equipment we have got it means that the measured hydraulic conductivity of the test section should be one or more orders of magnitude larger than the typical conductivity of the rock. This means a fracture transmissivity in the range of $T = > 10^{-7} \text{ m}^2/\text{s}$ for the target fracture. According to the prediction¹ there is a reasonable probability to encounter fractures with this transmissivity in the experiment area. The predicted median distance between them in boreholes is less than 10 m.

Fracture extension. It can be shown that a large transmissivity determined in a test also likely corresponds to an effective cross fracture transmissivity over a large fracture area³. It may thus be inferred that a transmissive fracture also has an extension that is larger than the median.

Geophysical signature. In order to identify the target fracture at earliest possible stage it is desirable that they can be detected by some geophysical method, i.e. borehole-radar.

Investigations in the Fracture Zone Crossing Exercise⁴ have shown that this may be possible with single fractures of the NNW-set.

If these demands are summarized the target fracture probably will be a **steeply dipping** fracture of the NNW-set with a transmissivity of $T=10^{-7}$ - 10^{-6} m²/s.

4 Transmissivity distribution

Many authors^{3,5} have found or assumed a lognormal distribution of the fracture transmissivity over the fracture plane. Very few actual measurements of this local transmissivity distribution has been performed. Most authors therefore use measurements of the aperture and from this calculates a local transmissivity by the cubic law. This is, however, not without objections since in many cases a discrepancy is shown between the calculated conductive and porous fracture openings. This discrepancy may be caused by channeling, fracture fillings, rock debris etc. The assumption that the transmissivity is lognormally distributed gives however some computational advantages, and since no data speak against this the assumption is kept in the conceptual model.

Flow theoretical considerations⁶ give that the cross fracture transmissivity, T_f , is equal to the geometric mean of the local fracture transmissivities. This means that the geometric mean of the transmissivity distribution for the target fracture will be $T_g=3 \cdot 10^{-7}$ m²/s.

The log standard deviation, $S_{\ln(T)}$, must be estimated in some indirect way. If we for this purpose go out from the cubic law, we find that the standard deviation of the log fracture transmissivity will be three times that of the aperture $S_{\ln(b)}$. Some values of $S_{\ln(b)}$ can be found in the literature giving approximate values from 0.5^{3,7} to 1⁸. The standard deviation of the point transmissivity would then be in the range of 0.5 to 3. For the conceptual model the values $S_{\ln(T)}=0, 0.5, 1$ and 2 should be tried.

Another question of importance is the autocorrelation structure of the fracture transmissivity. Very few data of this kind are published. The question is discussed by Geier et al³ and based on Stripa data they calculate a most likely correlation length of 2.15 cm. A more intuitive way of estimating the correlation length is to look at the "grain size" or "wave length" of the irregularities of a parameter over a domain. Aperture plots shown by Hakami⁶ do not speak against a typical wave length of 4 - 5 cm which would confirm a **correlation length** of a spherical variogram of 2 - 2.5 cm.

5 Fracture aperture

The fracture transmissivity is related to the aperture by the cubic law:

$$T = \rho \cdot g / \mu \cdot (b^3 / 12) \quad (1)$$

Several investigations have, however shown a discrepancy between the flow aperture and the porous aperture calculated from tracer test data. The general results are that the porous aperture is larger than the transmissive. This has been explained by flow tortuosity, weak sorbtion, matrix

diffusion, stagnant pools etc. Microslides of resin filled fractures⁹ have, however revealed that the fractures are very often filled with flakes of rock debris, that make them more complicated than a single slot with varying aperture, see Figure 5.1.

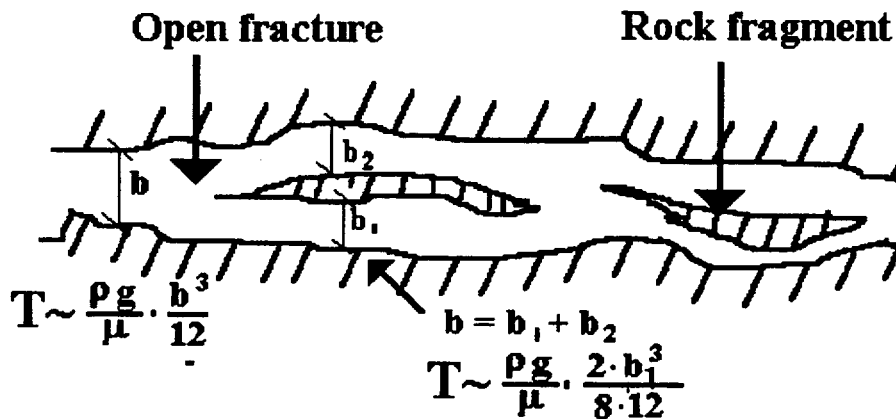


Figure 5.1 Fracture with rock fragments

For the single open slot the ratio between the pore volume and the transmissivity is

$V/T = \mu/\rho g * 12/b^2$ If the total available aperture for a fracture with a rock flake in is b , the ratio will be increased to $V/T = \mu/\rho g * 48/b^2$, if the pathways on each side of the flake have the same aperture, Thus a fourfold increase of the ratio. Obstructions in the fracture thus have a larger influence on the transmissivity compared to the porosity. Data on the effects of this on tracer transport are not available, but it may be worthwhile to try to simulate this in the scoping calculations for the MWTE. One can assume that the size of the portions with two or more branches are about the same size as the correlation length for the log transmissivity or about 2 - 3 cm. In the model the branching should be simulated with thin flakes situated in the middle of the fracture, see Figure 5.2.

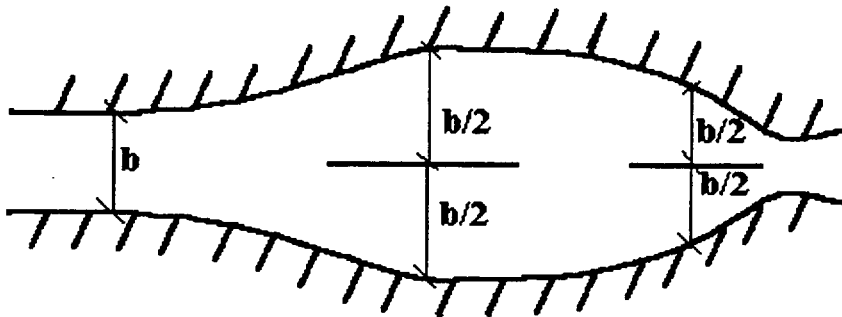


Figure 5.2. The simulated fracture geometry.

Simulations should be performed with 0, 10 and 20% of the fracture plane filled with flakes. Flake positions should be lumped over the plane. In further simulations correlated flake positions and transmissivity etc could be tried.

6 Summary of generic fracture properties

A summary of the properties of the generic fracture for the scoping calculation for the MWTE is given in table 6.1 below.

Table 5.1 Generic fracture properties for MWTE

Transmissivity: Lognormal distribution $T_g = 3 \cdot 10^{-7} \text{ m}^2/\text{s}$. $S_{\ln(T)} = 0, 0.5, 1 \text{ and } 2$

Correlation length: 2.5 cm with spherical isotropic variogram of $\ln(T)$

Aperture: Determined by cubic law Flake filling of 0, 10 and 20% of the surface

Fracture area: 200 x 200cm

7 References

¹Gustafson G et al, 1991: "Äspö Hard Rock Laboratory. Predictions prior to excavation and the process of their validation". SKB TR 91-23, Stockholm

²Olsson, O, 1993: "ÄHRL - Test plans for the operation phase". Material for the Scientific Advisory Committee in Kalmar, June 1993, Stockholm.

³Geier J E et al, 1992: "Discrete fracture modelling of the Finnsjön rock mass: Phase 2". SKB TR 92-07, Stockholm.

⁴Olsson O, 1992: "Characterization ahead of the tunnel front by radar and seismic methods - a case history from the Äspö Hard Rock Laboratory". SKB PR 25-92-01, Stockholm.

⁵Follin S, 1992: "Numerical simulation of double-packer tests in heterogeneous media", Dep. of engineering Geology, Lund Institute of Technology, Lund

⁶Dagan G, 1979: "Models of flow in statistically homogeneous formations". Water Resources Research, Vol 15 No 1.

⁷Hakami E, 1988: "Water flow in single rock joints". Licentiate thesis, Division of Rock Mechanics, Luleå University of Technology, Luleå.

⁸Gale J E, 1987: "Comparison of coupled fracture deformation and fluid flow models with direct measurements of fracture pore structure and stress-flow properties". 21th US Symp. on Rock Mechanics, Tucson, Arizona.

⁹Gale J E et al 1990: "Site Characterization and Validation - Measurement of Flowrate, Solute Velocities and Aperture Variation in Natural Fractures as a Function of Normal and Shear Stress, Stage 3". OECD/NEA Stripa Project PR 90-11, SKB, Stockholm.

APPENDIX B

Documentation of software and hardware.

Comment: The information given in this appendix will probably not support a "soft repeat", as intended. A SKB-project (called Documentation of the PHOENICS-code) is however in progress. The documentation from this project and the information in this appendix will provide for a "soft repeat" of calculations.

SKB - ÄSPÖ HARD ROCK LABORATORY

Documentation of numerical simulation by ...Urban..Svensson..(US).....1994-03-18...

Name

Date

OBJECT

SKB purchase order no: 8-10-180

Title of SKB purchase order: "Multiple Well Tracer Experiment" (MWTE)

Author of report: US

Company: CFE AB

Operator of computer and software: US

Company: CFE AB

COMPUTER

Name and version: Silicon Graphics Indigo, R 3000, entry level.

SOFTWARE

Operative system: IRIX 4

Code name: PHOENICS 1.6

Main manual: TR 100

Program language: FORTRAN

Compiler: F77 for IRIX 4

Preprocessor name:

Manual:

Postprocessor name:

Manual:

Subroutine:

Report: See

Subroutine:

Report: Kuylenstierna, Svensson

Subroutine:

Report: in the reference list.

CODE VERIFICATION

.. Distributor Not summarized in a single document.

Report/article:

Report/article:

Other verification

Report/article: Some verification in this report.

Report/article:

INPUT DATA

Ref: All in the report.

Ref:

Ref:

Ref:

Data file name:

Date of issue:

Stored at:

Data file name:

Date of issue:

Stored at:

Data file name:

Date of issue:

Stored at:

RESULTS

Report/article: In the report.

Report/article:

Data file name:

Stored at:

Data file name:

Stored at:

Data file name:

Stored at:

INFORMATION TO BE APPENDED TO WRITTEN DOCUMENT OF RESULTS

List of International Cooperations Reports

ICR 93-01

**Flowmeter measurement in
borehole KAS 16**
P Rouhiainen
June 1993
Supported by TVO, Finland

ICR 93-02

**Development of ROCK-CAD model
for Äspö Hard Rock Laboratory site**
Pauli Saksa, Juha Lindh,
Eero Heikkinen
Fintact KY, Helsinki, Finland
December 1993
Supported by TVO, Finland

ICR 93-03

**Scoping calculations for the Matrix
Diffusion Experiment**
Lars Birgersson¹, Hans Widén¹,
Thomas Ågren¹, Ivars Neretnieks²,
Luis Moreno²
1 Kemakta Konsult AB, Stockholm,
Sweden
2 Royal Institute of Technology,
Stockholm, Sweden
November 1993
Supported by SKB, Sweden

ICR 93-04

**Scoping calculations for the Multiple
Well Tracer Experiment - efficient design
for identifying transport processes**
Rune Nordqvist, Erik Gustafsson,
Peter Andersson
Geosigma AB, Uppsala, Sweden
December 1993
Supported by SKB, Sweden

ICR 94-01

**Scoping calculations for the Multiple
Well Tracer Experiment using a variable
aperture model**
Luis Moreno, Ivars Neretnieks
Department of Chemical Engineering
and Technology, Royal Institute of
Technology, Stockholm, Sweden
January 1994
Supported by SKB, Sweden

ICR 94-02

**Äspö Hard Rock Laboratory. Test plan for
ZEDEX - Zone of Excavation Disturbance
EXperiment. Release 1.0**

February 1994

Supported by ANDRA, NIREX, SKB

ISSN 1104-3210
ISRN SKB-ICR--9413--SE
CM Gruppen AB, Bromma 1994